

Fatigue Analysis of Connecting Rod Using Finite Element Analysis to Explore Weight and Cost Reduction Opportunities for a Production of Forged Steel Connecting Rod

Ambrish Tiwari, Jeetendra Kumar Tiwari, Sharad Kumar Chandrakar

³*Mechanical Engineering,
Shri Shankaracharya Group of Institute, Bhilai*

Abstract

The automobile engine connecting rod is a high volume production, critical component which subjects cyclic loaded during the Internal Combustion Engines (ICE) operation, it means that fatigue phenomena should be taken into account during the development, in order to guarantee the connecting rod required lifetime. Numerical tools have been extremely used during the connecting rod development phase, therefore, the complete understand of the mechanisms involved as well as the reliability of the numerical methodology are extremely important to take technological advantages, such as, to reduce project lead time and prototypes cost reduction. The present work shows the complete connecting rod Finite Element Analysis (FEA) methodology to explore weight and cost reduction opportunities for a production of forged steel connecting rod. It was also performed a fatigue study based on Stress Life (SxN) theory, considering the Modified Goodman diagram.

Keywords: Quasidynamic finite element analysis, fracture crackability, R ratio, optimization study.

1. Introduction

The automobile engine connecting rod is a high volume production, critical component. It connects reciprocating piston to rotating crankshaft, transmitting the thrust of the piston to the crankshaft. Every vehicle that uses an internal combustion engine requires at least one connecting rod depending upon the number of cylinders in the engine. Due to its large volume production, it is only logical that optimization of the connecting rod for its weight or volume will result in large-scale savings. It can also achieve the objective of reducing the weight of the engine component, thus

reducing inertia loads, reducing engine weight and improving engine performance and fuel economy.

Connecting rods for automotive applications are typically manufactured by forging from either wrought steel or powdered metal. They could also be cast. However, castings could have blow-holes which are detrimental from durability and fatigue points of view. The fact that forgings produce blow-hole-free and better rods gives them an advantage over cast rods. Between the forging processes, powder forged or drop forged, each process has its own pros and cons. Powder metal manufactured blanks have the advantage of being near net shape, reducing material waste. However, the cost of the blank is high due to the high material cost and sophisticated manufacturing techniques. With steel forging, the material is inexpensive and the rough part manufacturing process is cost effective. Bringing the part to final dimensions under tight tolerance results in high expenditure for machining, as the blank usually contains more excess material.

The main objective of this study was to explore weight and cost reduction opportunities for a production forged steel connecting rod. This has entailed performing a detailed load analysis. Therefore, this study has dealt with two subjects, first, dynamic load and quasi-dynamic stress analysis of the connecting rod. The loads acting on the connecting rod as a function of time were obtained. The relations for obtaining the loads and accelerations for the connecting rod at a given constant speed of the crankshaft were also determined. Quasidynamic finite element analysis was performed at several crank angles. The stress-time history for a few locations was obtained. The difference between the static FEA, quasidynamic FEA was studied. Based on the observations of the quasi-dynamic FEA, static FEA and the load analysis results, the load for the optimization study was selected.

The results were also used to determine the variation of R-ratio, degree of stress multiaxiality, and the fatigue model to be used for analyzing the fatigue strength. The component was optimized for weight and cost subject to fatigue life and space constraints and manufacturability. It is the conclusion of this study that the connecting rod can be designed and optimized under a load range comprising tensile load corresponding to 360° crank angle at the maximum engine speed as one extreme load, and compressive load corresponding to the peak gas pressure as the other extreme load. Furthermore, the existing connecting rod can be replaced with a new connecting rod made of C-70 steel that is 10% lighter and 25% less expensive due to the steel's fracture crackability. The fracture crackability feature, facilitates separation of cap from rod without additional machining of the mating surfaces. Yet, the same performance can be expected in terms of component durability.

FEA WITH DYNAMIC LOADS

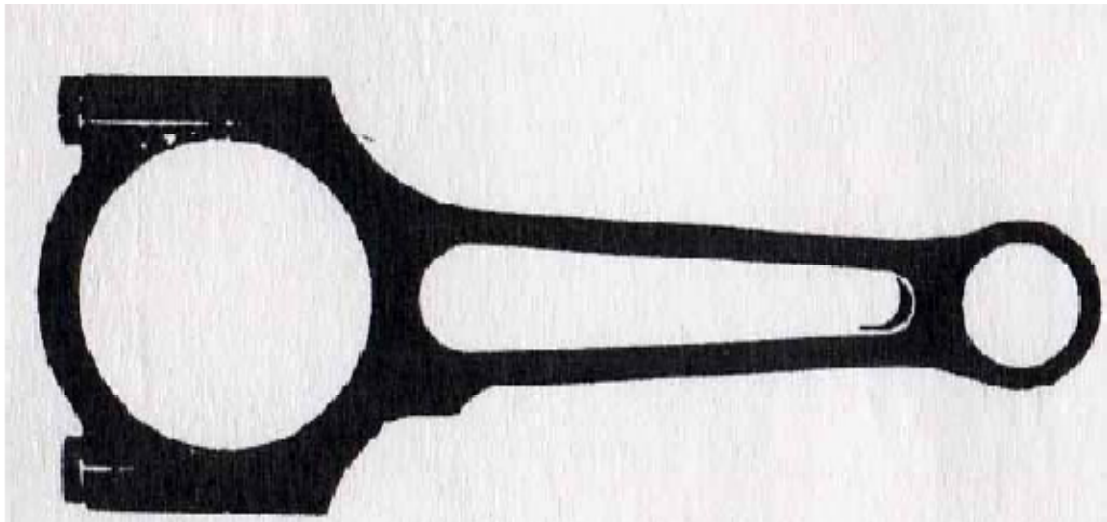


Fig 1: Design of a PM connecting rod (Sonsino and Esper, 1994).

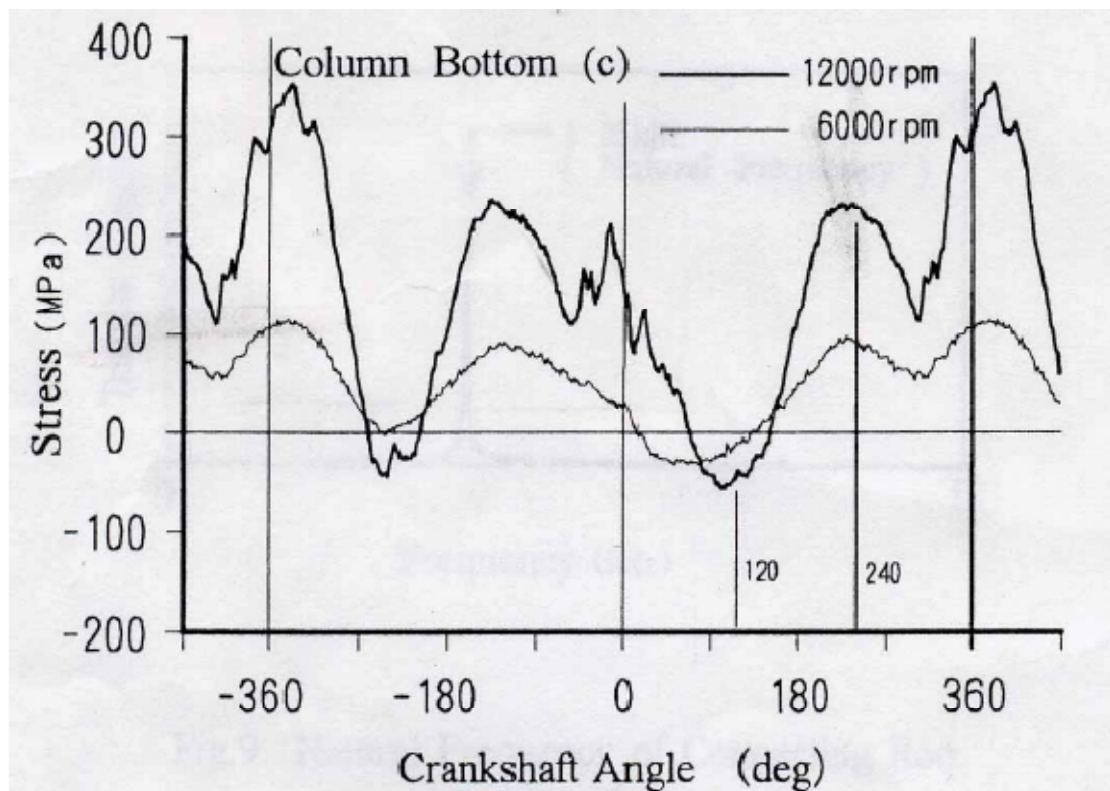


Fig 2: Stresses at the bottom of the connecting rod column (Ishida et al., 1995).

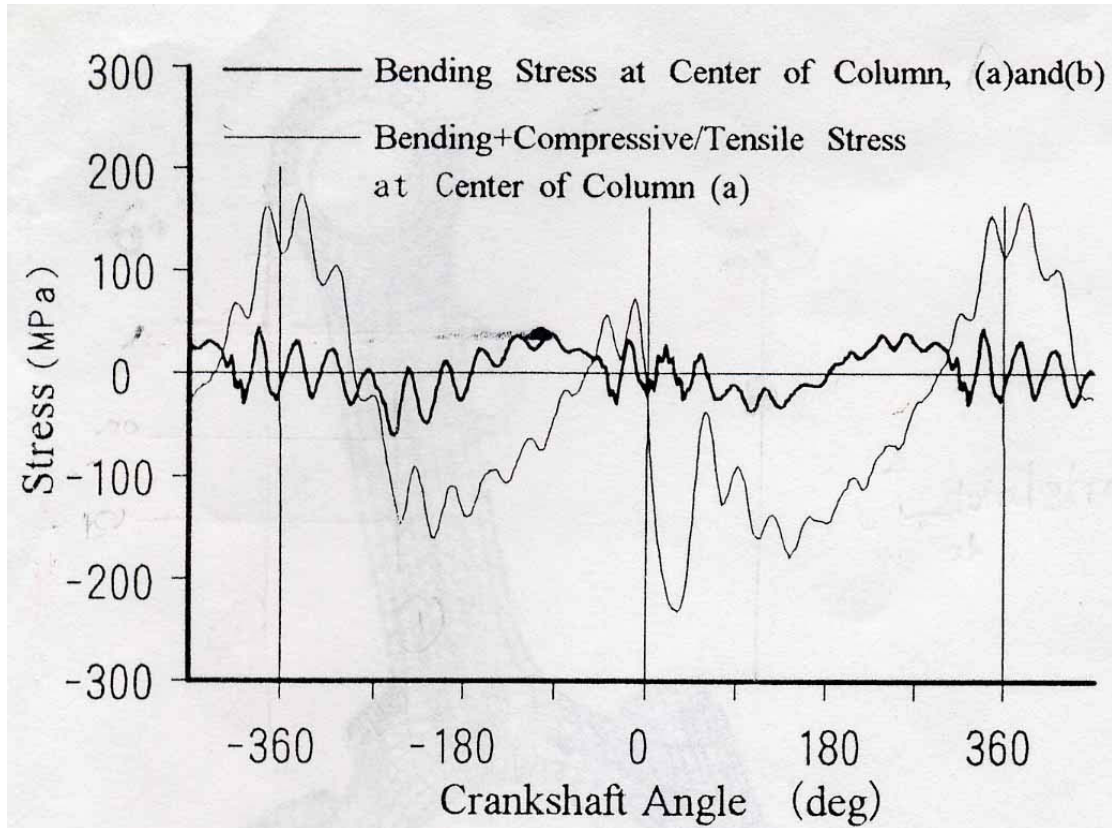


Fig 3: Stresses at the center of the connecting rod column (Ishida et al., 1995).

Once the components of forces at the connecting rod ends in the X and Y directions are obtained, they can be resolved into components along the connecting rod length and normal to it. The components of the inertia load acting at the center of gravity can also be resolved into similar components. It is neither efficient nor necessary to perform FEA of the connecting rod over the entire cycle and for each and every crank angle. Therefore, a few positions of the crank were selected depending upon the magnitudes of the forces acting on the connecting rod, at which FEA was performed. The justification used in selecting these crank positions is as follows:

The stress at a point on the connecting rod as it undergoes a cycle consists of two components, the bending stress component and the axial stress component. The bending stress depends on the bending moment, which is a function of the load at the C.G. normal to the connecting rod axis, as well as angular acceleration and linear acceleration component normal to the connecting rod axis. The variation of each of these three quantities over 0° – 360° is identical to the variation over 360° – 720° . This can be seen from Figure given below for the normal load at the connecting rod ends and at the center of gravity. In addition, Figure below shows identical variation of angular acceleration over 0° – 360° and 360° – 720° .

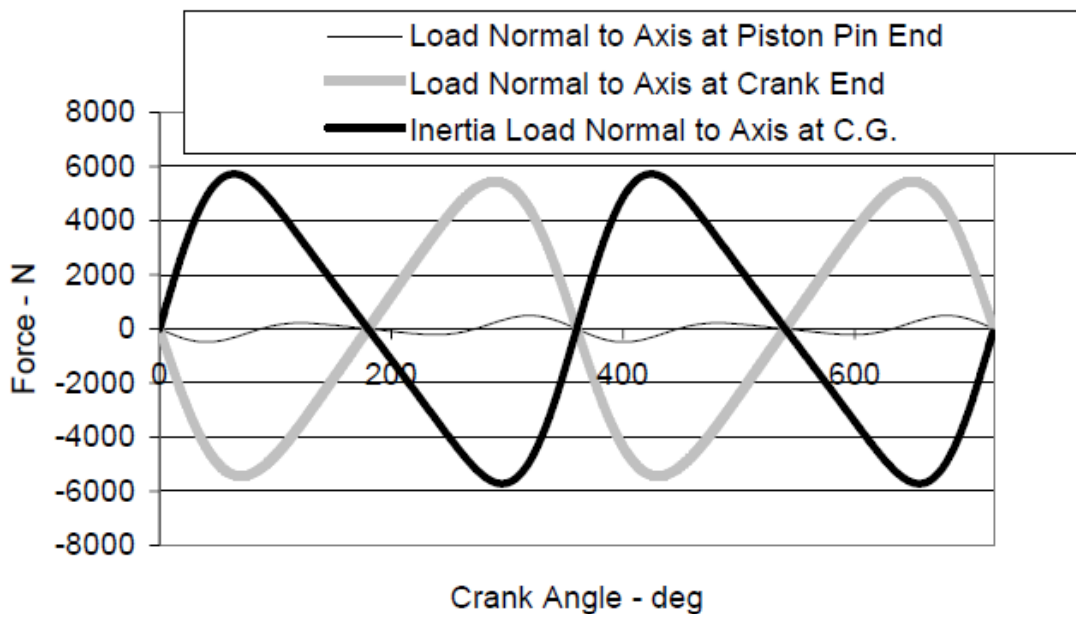


Fig 4: Loads normal to the connecting rod axis. Note that variations from 0° to 360° repeat from 360° to 720°.

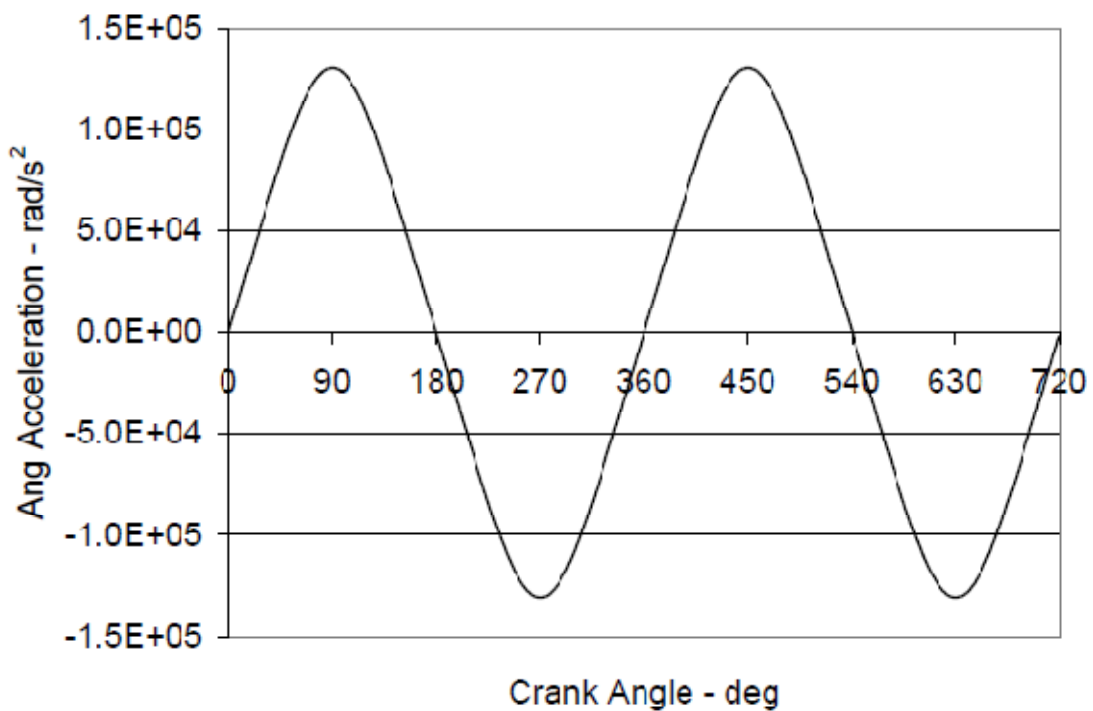


Fig 5: Variation of angular acceleration of the connecting rod over one complete engine cycle at crankshaft speed of 5700 rev/min.

Therefore, for any given point on the connecting rod the bending moment varies in an identical fashion from 0° – 360° crank angle as it varies from 360° – 720° crankangle.

The axial load variation, however, does not follow this repetitive pattern. (i.e one cycle of axial load variation consists of the entire 720°). This is due to the variation in the gas load, one cycle of which consists of 720° . However, the variation over 0° – 360° can be superimposed with the variation over 360° – 720° and this plot can be used to determine the worst of the two cycles of 0° – 360° and 360° – 720° to perform FEA, as shown in Figure below

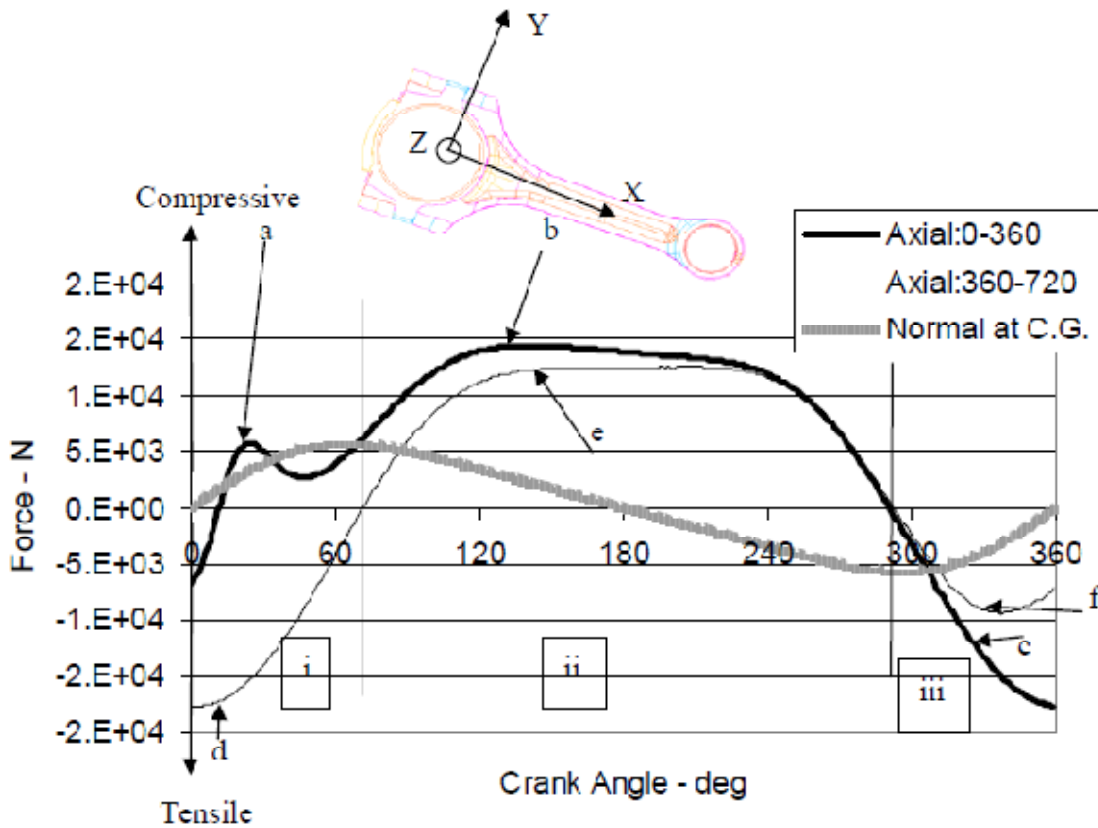


Fig 6: Variation of the axial load at the crank end and the load normal to connecting rod length at the C.G. at 5700 rev/min crankshaft speed. The 360° to 720° variation has been superimposed on 0° to 360° variation. Plot has been divided into three regions: i, ii and iii.

In this figure, a point on the “Axial: 360-720” curve, say at 20° crank angle, actually represents $360^{\circ} + 20^{\circ}$ or 380° crank angle. The axial load at the crank end and at the piston pin end are not generally identical at any point in time. They differ due to the inertia load acting on the connecting rod. The load at either end could be used as a basis for deciding points at which to perform FEA. The load at the crank end was used in this work.

The stress at any point on the connecting rod at this axial load can be interpolated from the axial stress analysis results. Results of the FEA are discussed in Tables 2.3, 2.4, and 2.5 list the crank angles at which FEA was performed at 5700 rev/min, 4000 rev/min, and 2000 rev/min, respectively. Parameters that are needed to perform FEA using I-DEAS are also listed in these tables.

If the axial component of the load at the crank end or pin end was tensile the load was applied with a cosine distribution, while if the axial component of the load was compressive the load was applied with uniform distribution.

Table1: Inputs for FEA of connecting rod using dynamic analysis results at crankshaft speed of 5700 rev/min.

Crank Angle	Ang. Velocity	Ang. Accln	Crank End Load				Piston Pin End Load				Pressure Constant for UDL -(MPa)		Pressure Constant for Cosine Load-(MPa)	
			F _{AX}	F _{AY}	Resultant	Direction	F _{BX}	F _{BY}	Resultant	Direction	Crank End	Pin End	Crank End	Pin End*
deg	rev/s	rev/s ²	N	N	N	deg	N	N	N	deg				
0	-32.7	0	-6832	0	6832	0.0	-1447	0	1447	0.0		3.8	10.6	
24	-30.1	7205	5330	-3698	6487	-34.8	-12744	1405	12821	-6.3	9.1	33.6		
60	-17.1	17119	2174	-6254	6621	-70.8	-5639	1371	5803	-13.7	9.3	15.2		
126	20.0	15699	12736	-7121	14592	-29.2	-8070	2559	8466	-17.6	20.6	22.2		
180	32.7	0	13856	0	13856	0.0	-6929	0	6929	0.0	19.5	18.2		
243	15.6	-17765	9891	7189	12228	36.0	-6037	-2166	6414	19.7	17.2	16.8		
288	-10.7	-19380	-815	5470	5530	-81.5	-964	-107	970	6.3	7.8	2.5		
336	-30.1	-7205	-14997	826	15020	-3.2	7584	1467	7724	10.9			23.4	23.2
360	-32.7	0	-17683	0	17683	0.0	9404	0	9404	0.0			27.5	28.3
396	-32.3	2702	-17485	-212	17487	0.7	9330	-670	9354	-4.1			27.2	28.1
432	-10.7	19380	-1585	-5203	5439	73.1	-194	-159	251	39.4	7.7	0.7		
486	20.0	15699	10275	-6408	12109	-31.9	-5609	1846	5905	-18.2	17.1	15.5		
696	-30.1	-7205	-9625	1585	9755	-9.4	2211	708	2322	17.8			15.2	7.0

Table2: Inputs for FEA of connecting rod using dynamic analysis results at crankshaft speed of 4000 rev/min.

Crank Angle	Ang. Velocity	Ang. Accln	Crank End				Piston Pin End				Pressure Constant for UDL -(MPa)		Pressure Constant for Cosine Load-(MPa)	
			F _{AX}	F _{AY}	Resultant	Direction	F _{BX}	F _{BY}	Resultant	Direction	Crank End	Pin End	Crank End	Pin End*
deg	rev/s	rev/s ²	N	N	N	deg	N	N	N	deg				
23	-21.3	3401	13579	-3237	13960	-13.4	-17265	2152	17398	-7.1	19.69	45.60		
24	-21.2	3548	13477	-3354	13888	-14.0	-17128	2225	17272	-7.4	19.59	45.27		
126	14.0	7731	7749	-3934	8691	-26.9	-5451	1688	5707	-17.2	12.26	14.96		
360	-22.9	0	-8366	0	8366	0.0	4289	0	4289	0.0			13.01	12.88
362	-22.9	296	-8406	-26	8406	0.2	4332	-71	4333	-0.9			13.07	13.01

Table3: Inputs for FEA of connecting rod using dynamic analysis results at crankshaft speed of 2000 rev/min.

Crank Angle	Ang. Velocity	Ang. Accln	Crank End				Piston Pin End				Pressure Constant for UDL -(MPa)		Pressure Constant for Cosine Load-(MPa)	
			F _{AX}	F _{AY}	Resultant	Direction	F _{BX}	F _{BY}	Resultant	Direction	Crank End	Pin End	Crank End	Pin End*
deg	rev/s	rev/s ²	N	N	N	deg	N	N	N	deg				
22	-10.7	813	19636	-2886	19847	-8.4	-20565	2626	20732	-7.3	27.99	54.34		
24	-10.6	887	19405	-3104	19652	-9.1	-20318	2822	20513	-7.9	27.72	53.77		
126	7.0	1933	4120	-1616	4425	-21.4	-3545	1054	3699	-16.6	6.24	9.69		
360	-11.5	0	-1586	0	1586	0.0	566	0	566	0.0			2.47	1.70
371	-11.3	407	-1684	-62	1685	2.1	687	-70	691	-5.8			2.62	2.07

Acceleration at the crank end center is 2,127,448 mm/s².

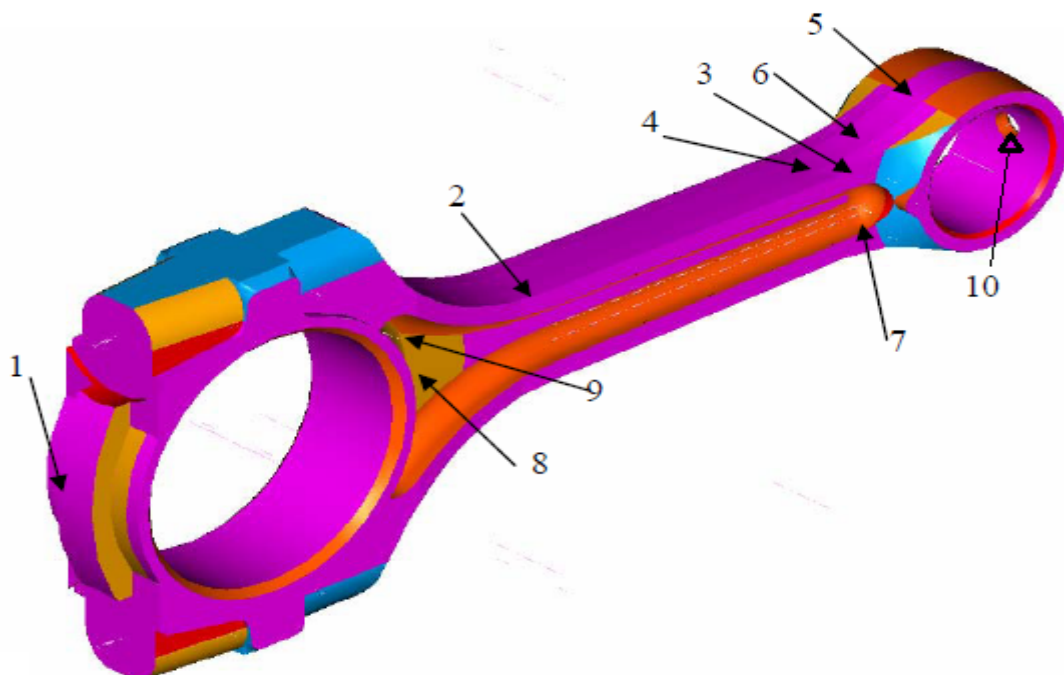
Pressure constant for UDL as defined by Equation 3.6.

Pressure constant for cosine load as defined by Equation 3.3.

* The pressure constants in this column have been corrected for the oil hole

Static FEA

Finite element mesh was generated using parabolic tetrahedral elements with various element lengths of 2.5 mm (20719 elements), 2 mm (37373 elements), 1.5 mm (77316 elements), and 1 mm (226409 elements). The von Mises stress was checked for convergence at ten locations, as shown in figure



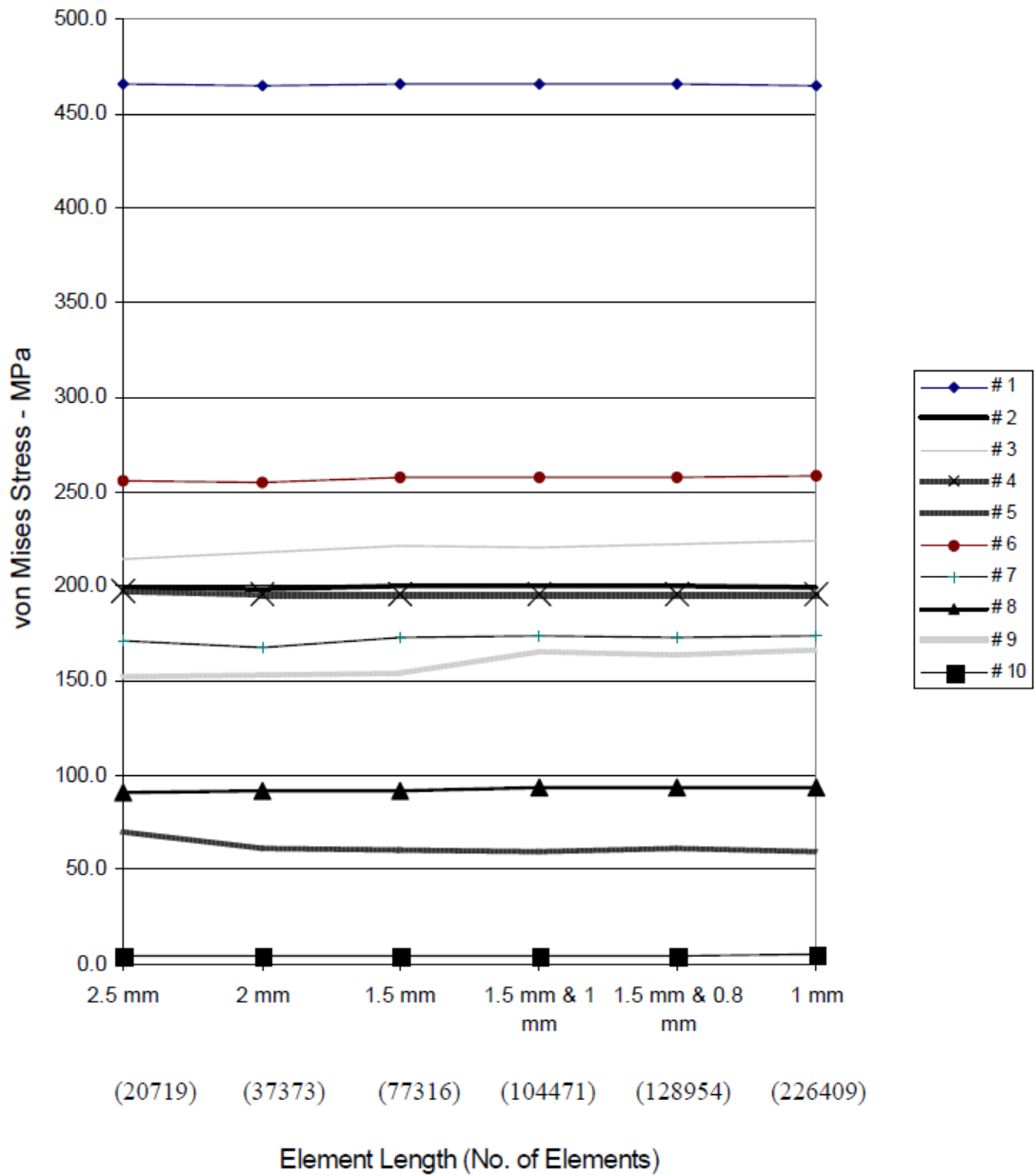


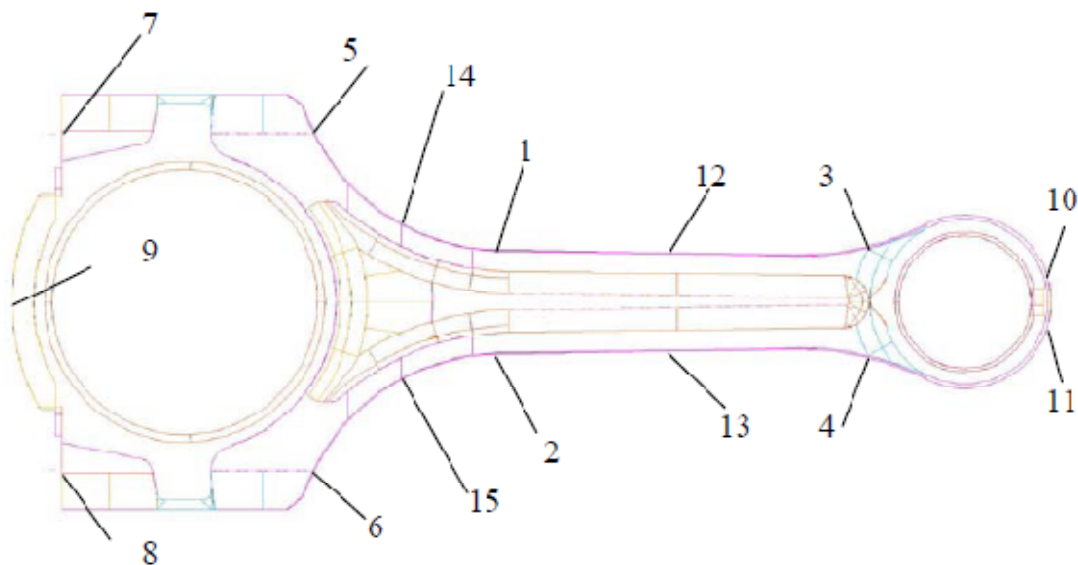
Fig7: von Mises stress at locations 1 through 10 in Note that convergence is achieved at most locations with element length of 1.5 mm. Further local refinement with element length of 1 mm produced convergence at location 9.

For most areas on the connecting rod convergence has been achieved with 1.5 mm uniform element length. This is evident for all locations, except 9, in Figure. Therefore, a finite element mesh was generated with a uniform global element length of 1.5 mm, and at locations with chamfers a local element length of 1 mm was used. This resulted in a mesh with 104471 elements. Further refinement was done locally by

using element length of 0.8 mm (128954 elements). It can be seen that convergence has been achieved with 1 mm local mesh size. The maximum percentage difference between the stress values observed between the last two models (the one with 104471 elements and the one with 128954 elements) is 2.3%, which is small. Hence, the mesh with 104471 elements was used for FEA.

Quasi-Dynamic FEA

The same mesh that was used for static FEA, as presented in the section above, was also used for quasi-dynamic FEA. Convergence was checked at locations where high bending stresses are expected. In this case they were checked at locations 12 and 13, about 87.6 mm from crank end center, as shown in Figure below



As discussed, locations 12 and 13 experience considerably high bending stresses. Figure below indicates that convergence of stress σ_{xx} was achieved with a mesh that uses 1.5 mm uniform global element length and 1 mm local element length

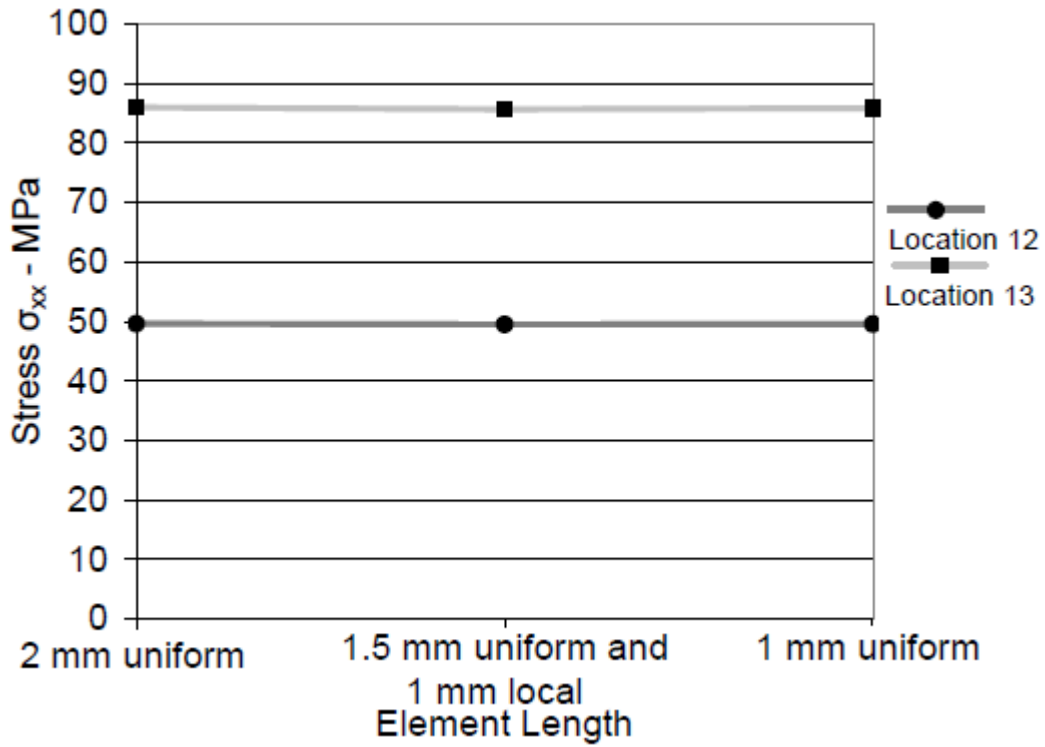


Fig 8: Stress along the connecting rod axis in the shank of the connecting rod under dynamic loads as a function of mesh size.

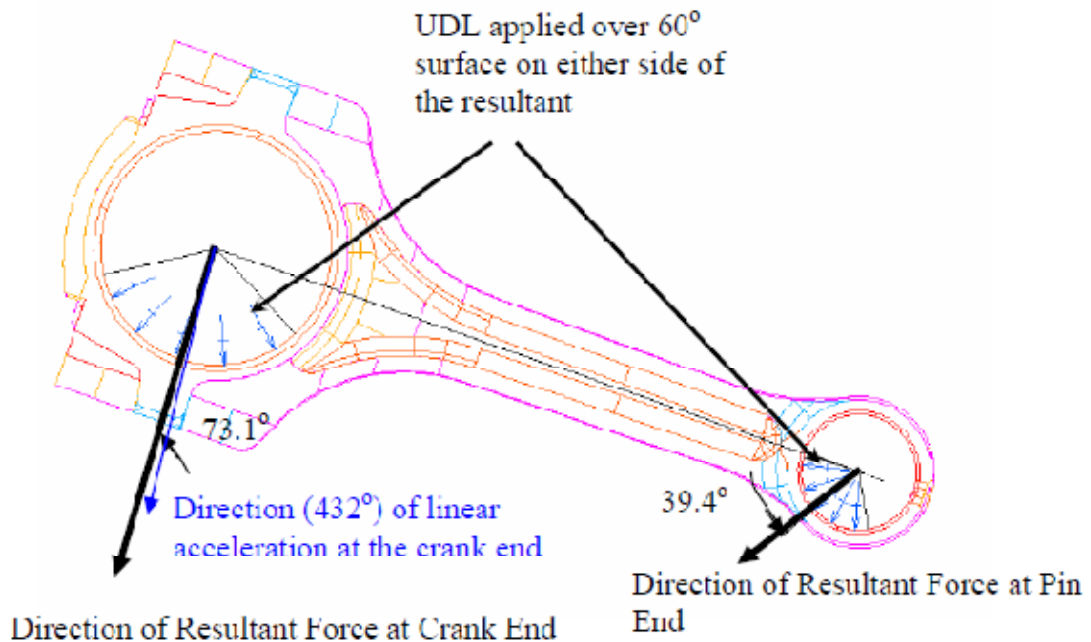


Fig 9: Illustration of the way in which boundary conditions were applied when solving the quasi-dynamic FEA model.

Test Assembly FEA

The mesh used for static FEA used 1.5 mm global element length and 1 mm local element length at chamfers. The mesh used for assembly FEA was even finer. The mesh was generated with an element length of 1 mm between the ends of the connecting rod and 1.5 mm at the cap. Since convergence was checked for the mesh used in static FEA

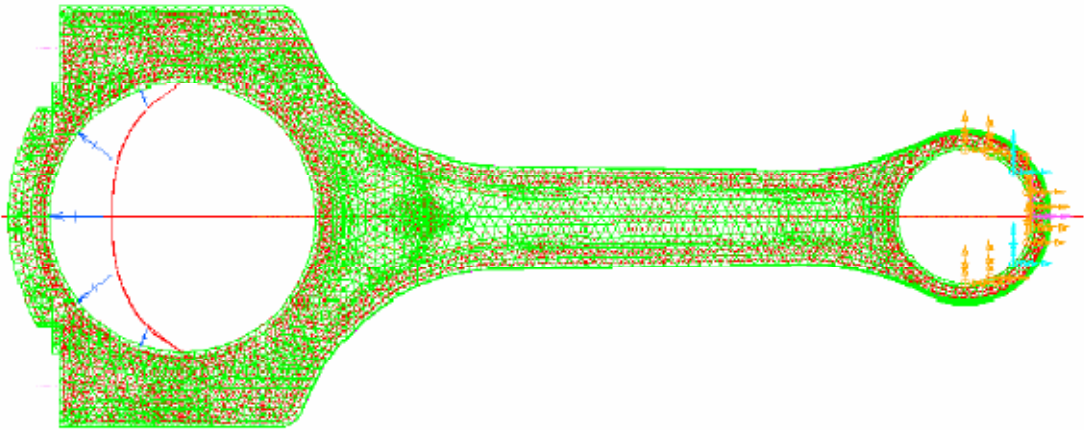


Fig 10: FEA model of the connecting rod with axial tensile load at the crank end with cosine distribution over 180° and piston pin end restrained over 180° .

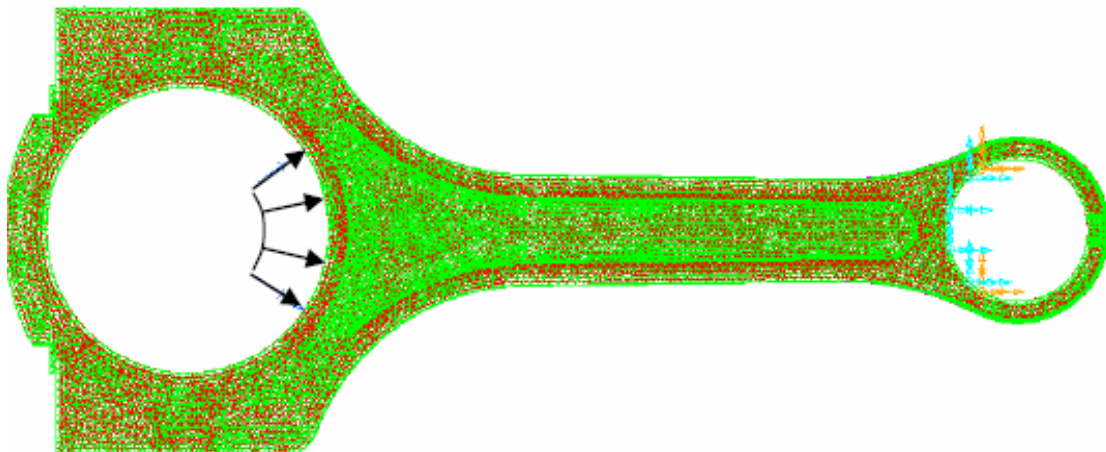


Fig 11: FEA model of the connecting rod with axial compressive load at the crank end uniformly distributed over 120° and piston pin end restrained over 120° .

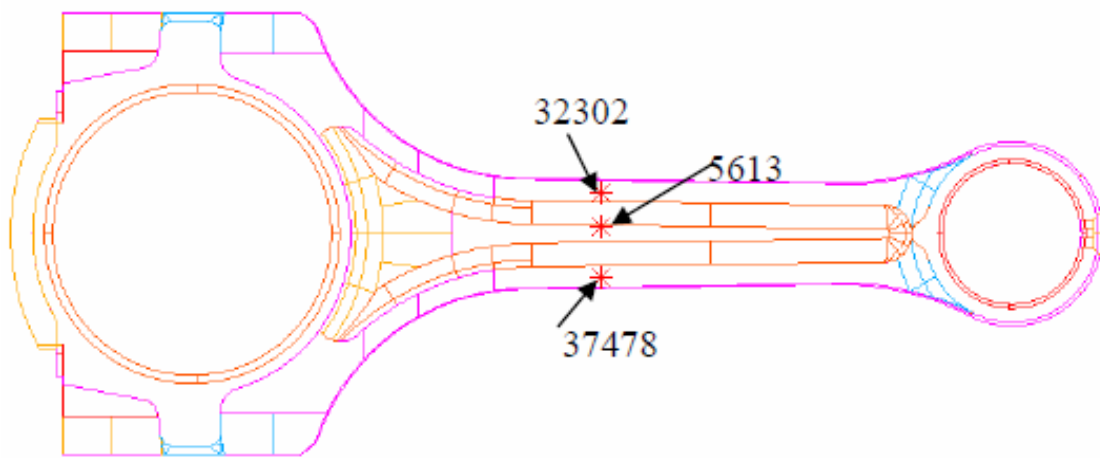


Fig 12: Location of nodes used for validation of the FEA model.

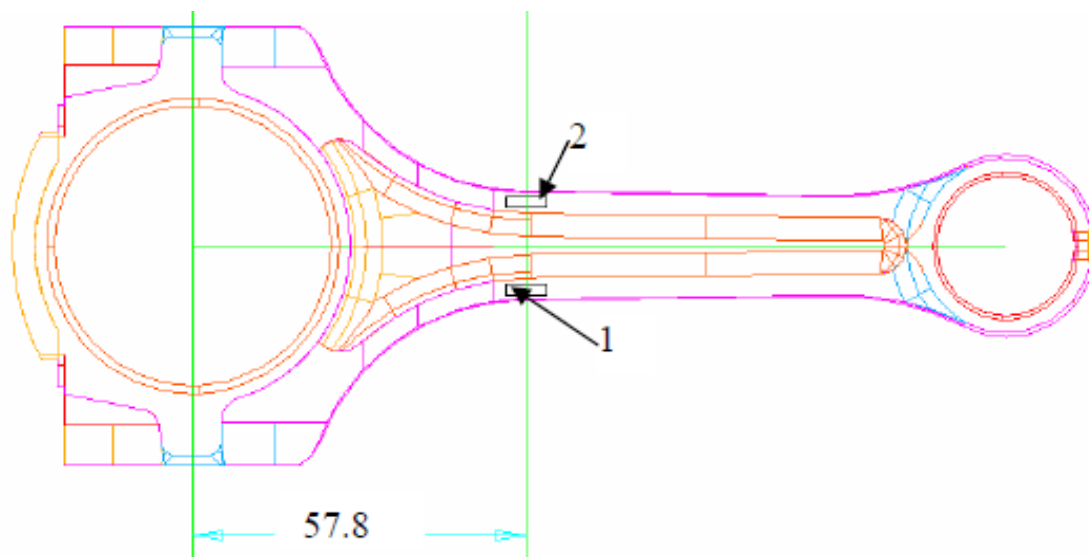


Fig 13: Location of two strain gages attached to the connecting rod. Two other gages are on the opposite side in identical positions.

COMPARISON OF STATIC AND QUASI-DYNAMIC FEA RESULTS

The maximum load of 17.72 kN at the crank end from the dynamic load analysis occurs at the crank angle of 360°. The load at the crank end at the crank angle of 360° is 17.68 kN, a difference of 0.2%. In Figure the von Mises stress at location 9 under a static load of 17.7 kN (the load at 360o crank angle) is superimposed with the stress variation under dynamic loads (service operating condition).

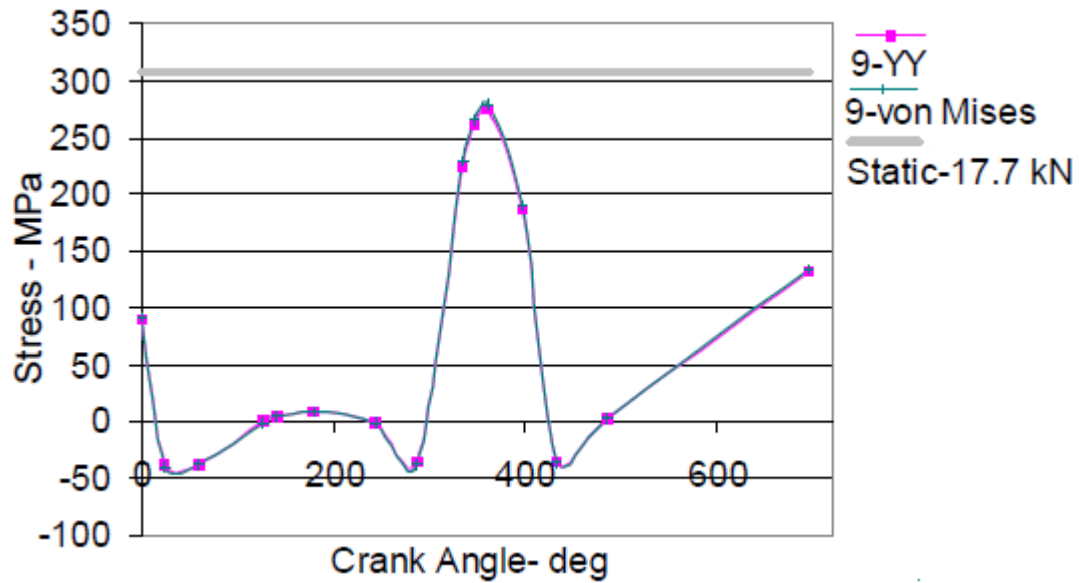


Fig 14: Stress variation over the engine cycle at 5700 rev/min at location 9. YY is the σ_{yy} component. The stress shown for the static tensile load of 17.7 kN is the von Mises stress.

Similar plots are provided for locations 5, 6, 7, and 8 Figures.

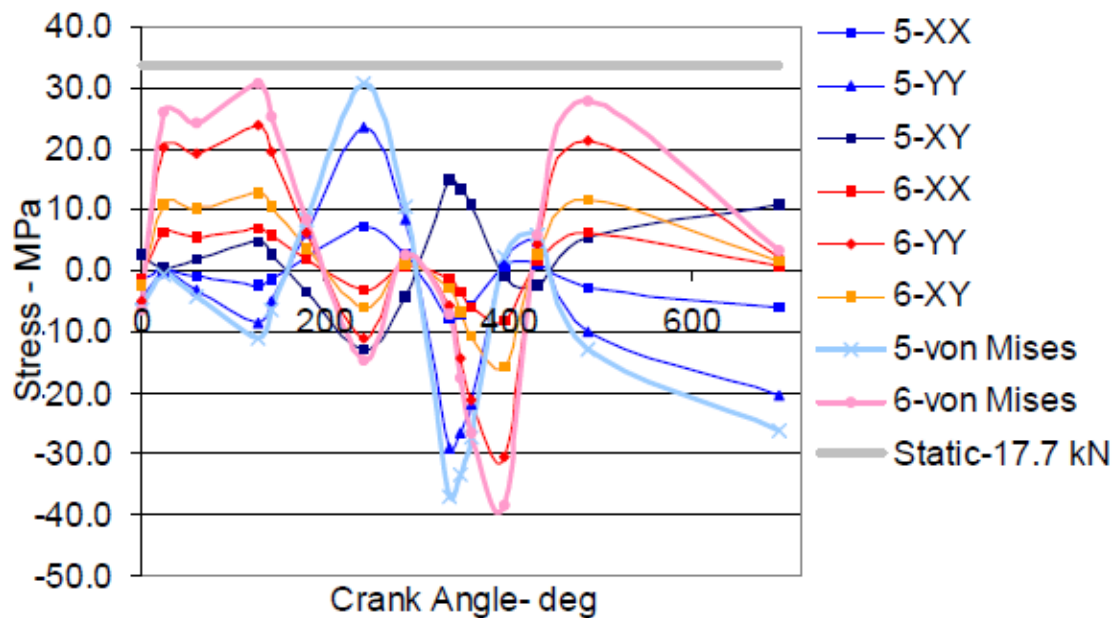


Fig 15: Stress variation over the engine cycle at 5700 rev/min at locations 5 and 6.

XX is the σ_{xx} component of stress, YY is the σ_{yy} component and so on. The stress shown for the static tensile load of 17.7 kN is the von Mises stress.

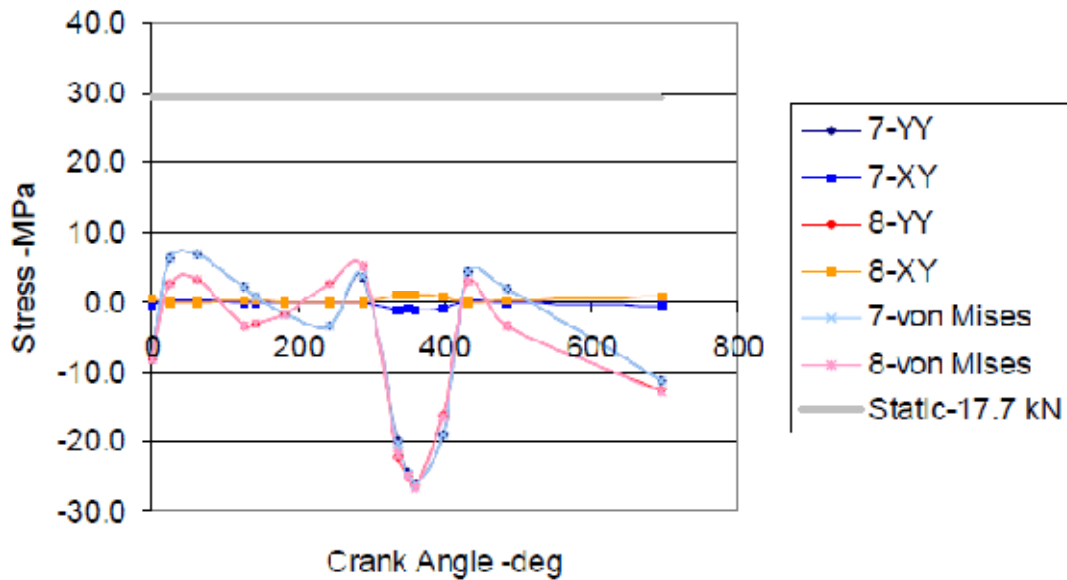


Fig 16: Stress variation over the engine cycle at 5700 rev/min at locations 7 and 8.

YY is the σ_{yy} component, XY is the σ_{xy} component of stress, and so on. The stress shown for the static tensile load of 17.7 kN is the von Mises stress.

Evidently, FEA under static load predicts higher stresses by about 10% at location 9 (compare maximum stress from quasi-dynamic FEA with static stress), which is one of the critical locations. Similar trend is observed for locations 5, 6, 7 and 8.

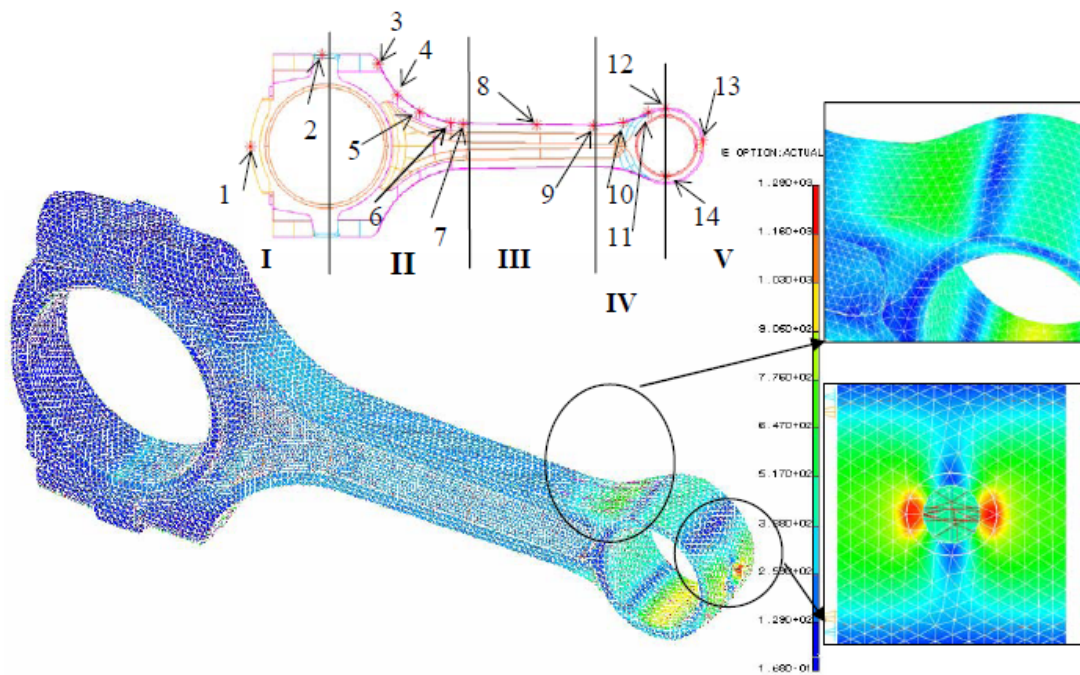


Fig 17: Von Mises stress distribution with static tensile load of 26.7 kN at piston pin end. The crank end was restrained.

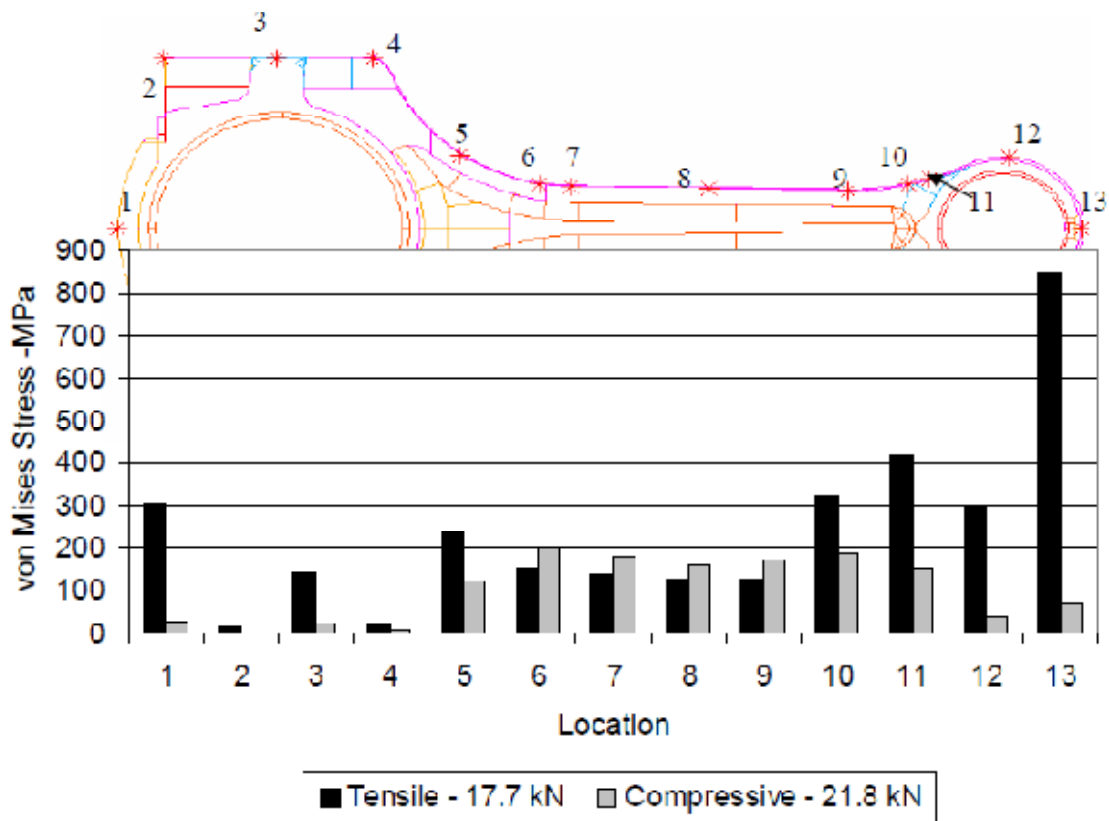


Fig 18: Von Mises stress at a few discrete locations on the mid plane labeled on the connecting rod, along the length, for tensile (17.7 kN) and compressive loads (21.8 kN).

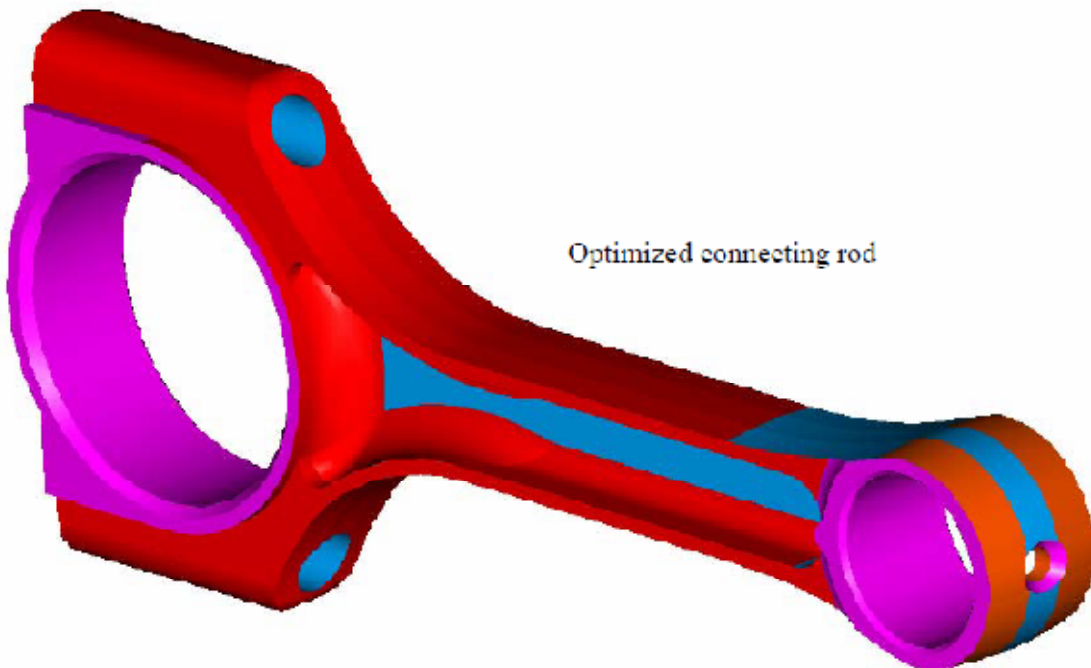
CONCLUSIONS

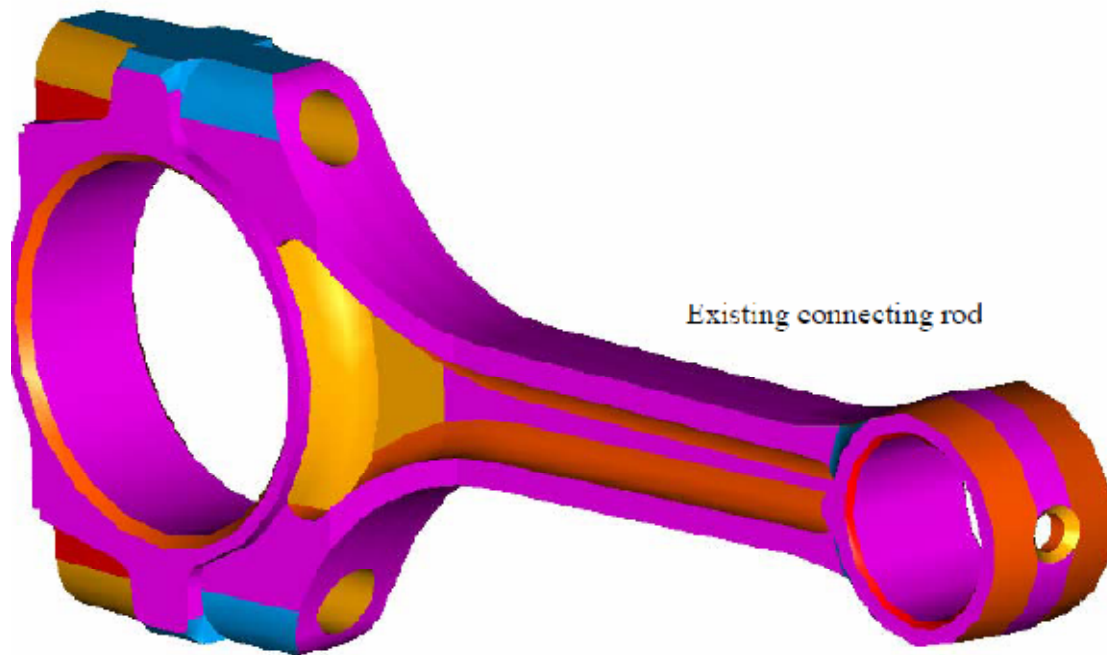
This research project investigated weight and cost reduction opportunities that steel forged connecting rods offer. The connecting rod chosen for this project belonged to a mid size sedan and was supplied by an OEM. First, the connecting rod was digitized. Load analysis was performed based on the input from OEM, which comprised of the crank radius, piston diameter, the piston assembly mass, and the pressure-crank angle diagram, using analytical techniques and computer-based mechanism simulation tools (IDEAS and ADAMS). Quasi-dynamic FEA was then performed using the results from load analysis to gain insight on the structural behavior of the connecting rod and to determine the design loads for optimization. The following conclusions can be drawn from this study:

- 1) There is considerable difference in the structural behavior of the connecting rod between axial fatigue loading and dynamic loading (service operating condition). There are also differences in the analytical results obtained from fatigue loading simulated by applying loads directly to the connecting rod and from fatigue loading with the pins and interferences modeled.
- 2) Dynamic load should be incorporated directly during design and optimization as the design loads, rather than using static loads. The load range comprising of the peak gas load and the load corresponding to 360° crank angle at 5700 rev/min (maximum engine speed) can be used for design and optimization (subject to verification for the particular engine), as the design loads.
- 3) Bending stresses were significant and should be accounted for. Tensile bending stresses were about 16% of the stress amplitude (entire operating range) at the start of crank end transition and about 19% of the stress amplitude (entire operating range) at the shank center. Bending stresses were negligible at the piston pin end. The R ratio (i.e. minimum to maximum stress ratio) varies with location on the connecting rod and with speed of the crankshaft. The stress ratio varies from -0.14 at the extreme end of the connecting rod cap to -1.95 at the crank end transition, under service operating conditions considering the entire load range. In the middle of the shank the R ratio varies from -18.8 at 2000 rev/min to -0.86 at 5700 rev/min.
- 4) The stress multiaxiality is high (the transverse component is 30% of the axial component), especially at the critical region of the crank end transition. Therefore, multiaxial fatigue analysis is needed to determine fatigue strength. Due to proportional loading, equivalent stress approach based on von Mises criterion can be used to compute the equivalent stress amplitude. Optimization was performed to reduce weight and manufacturing cost. Cost was reduced by changing the material of the current forged steel connecting rod to crackable forged steel (C-70). While reducing the weight, the static strength, fatigue strength, and the buckling load factor were taken into account. The

following conclusions can be drawn from the optimization part of the study:

- 1) Fatigue strength was the most significant factor (design driving factor) in the optimization of this connecting rod.
- 2) The connecting rod was optimized under a load range comprising the dynamic load at 360° crank angle at maximum engine speed and the maximum gas load. This connecting rod satisfied all the constraints defined and was found to be satisfactory at other crank angles also.
- 3) At locations like the cap-rod outer edge, the extreme end of the cap, and the surface of the piston pin end bore, the stresses were observed to be significantly lower under conditions of assembly (with bearings, crankshaft and piston pin and bushing), when compared to stresses predicted by cosine loading (tensile load).
- 4) The optimized geometry is 10% lighter and cost analysis indicated it would be 25% less expensive than the current connecting rod, in spite of lower strength of C-70 steel compared to the existing forged steel. PM connecting rods can be replaced by fracture splittable steel forged connecting rods with an expected cost reduction of about 15% or higher, with similar or better fatigue behaviour.
- 5) By using other fracture crackable materials such as micro-alloyed steels having higher yield strength and endurance limit, the weight at the piston pin end and the crank end can be further reduced. Weight reduction in the shank region is, however, limited by manufacturing constraints.





REFERENCES

- [1] Afzal, A., 2004, "Fatigue Behavior and Life prediction of Forged Steel and PM Connecting Rods," *Master's Thesis, University of Toledo*.
- [2] Athavale, S. and Sajanpawar, P. R., 1991, "Studies on Some Modelling Aspects in the Finite Element Analysis of Small Gasoline Engine Components," *Small Engine Technology Conference Proceedings, Society of Automotive Engineers of Japan, Tokyo*, pp. 379-389.
- [3] Balasubramaniam, B., Svoboda, M., and Bauer, W., 1991, "Structural optimization of I.C. engines subjected to mechanical and thermal loads," *Computer Methods in Applied Mechanics and Engineering*, Vol. 89, pp. 337-360.
- [4] Bhandari, V. B., 1994, "Design of Machine Elements," Tata McGraw-Hill.
- [5] Clark, J. P., Field III, F. R., and Nallicheri, N. V., 1989, "Engine state-of-the-art a competitive assessment of steel, cost estimates and performance analysis," *Research Report BR 89-1, Automotive Applications Committee, American Iron and Steel Institute*.
- [6] El-Sayed, M. E. M., and Lund, E. H., 1990, "Structural optimization with fatigue life constraints," *Engineering Fracture Mechanics*, Vol. 37, No. 6, pp. 1149-1156.
- [7] Folgar, F., Wldrig, J. E., and Hunt, J. W., 1987, "Design, Fabrication and Performance of Fiber FP/Metal Matrix Composite Connecting Rods," *SAE Technical Paper Series 1987*, Paper No. 870406.
- [8] Sonsino, C. M., and Esper, F. J., 1994, "Fatigue Design for PM Components," *European Powder Metallurgy Association (EPMA)*.

- [9] Stephens, R. I., Fatemi, A., Stephens, R. R., and Fuchs, H. O., 2000, "Metal Fatigue in Engineering," *2nd Edition, John Wiley and Sons, Inc.*
- [10] Webster, W. D., Coffell R., and Alfaro D., 1983, "A Three Dimensional Finite Element Analysis of a High Speed Diesel Engine Connecting Rod," *SAE Technical Paper Series, Paper No. 831322.*
- [11] Wilson, C. E. and Sadler, P. J., 1993, "Kinematics and Dynamics of Machinery," *2nd Edition, HarperCollins College Publishers.*
- [12] Yoo, Y. M., Haug, E. J., and Choi, K. K., 1984, "Shape optimal design of an engine connecting rod," *Journal of Mechanisms, Transmissions, and Automation in Design, Transactions of ASME, Vol. 106, pp. 415-419.*